
Multicellular Dosimetry for Micrometastases: Dependence of Self-Dose Versus Cross-Dose to Cell Nuclei on Type and Energy of Radiation and Subcellular Distribution of Radionuclides

S. Murty Goddu, Dandamudi V. Rao and Roger W. Howell

Department of Radiology, University of Medicine and Dentistry of New Jersey, New Jersey Medical School, Newark, New Jersey

In radioimmunotherapy, the treatment of bulk tumors by radionuclides that emit energetic beta particles is the preferred approach. However, for the eradication of small clusters of cancer cells, radionuclides that emit Auger electrons or alpha particles are considered to be advantageous because of their ability to deposit radiation energy locally. If such radionuclides are internalized by the cells, the total dose to the cell nuclei is thought to be primarily determined by the self-dose (dose to cell nucleus from activity within the cell) in comparison to the cross-dose (dose to the cell nucleus from activity in all other cells). **Methods and Results :** The self-dose-to-cross-dose ratios to the cell nucleus were calculated for different cluster sizes (26–400 μm) with monoenergetic electron and alpha particle sources distributed uniformly in different cell compartments (cell surface, cytoplasm, nucleus). Model calculations were also performed for several radionuclides (Auger, beta and alpha emitters). Absorbed fractions for sources of monoenergetic electron and alpha particles, distributed uniformly in small spheres (26–5000 μm), were also calculated along with S-values for a number of radionuclides. **Conclusions:** When most of the cells in the cluster are labeled with beta or alpha emitters, the cross-dose component of the total dose is important irrespective of cluster size and subcellular source distribution and increases as the cluster size increases. The self-dose is always important for Auger emitters. When the self-dose is negligible, the mean absorbed dose to the cell nuclei is well represented by the mean dose to the micrometastasis.

Key Words: dosimetry; micrometastases; radionuclides; radioimmunotherapy; absorbed fractions

J Nucl Med 1994; 35:521–530

The potential of radiolabeled immunoconjugates to selectively seek malignant cells and destroy them has attracted considerable attention, and has opened new ave-

nues of research in our fight against cancer. The outcome after radioimmunotherapy (RIT) of bulk tumors ($d > 1$ cm) with radiolabeled antibodies can be monitored by external imaging of the tumor using radiographic and nuclear medicine techniques (1) and correlated with the absorbed dose to the tumor. Such tumors are most effectively treated with radionuclides which emit energetic beta-particles because they effectively cross-irradiate the malignant tissue while depositing most of their energy in the tumor (2–6). In contrast to tumors of macroscopic dimensions ($d > 1$ cm), RIT of very small micrometastases ($d < 0.1$ cm) cannot be evaluated with external imaging techniques because of inherent resolution limitations of the imaging equipment. Consequently, approaches developed to treat small clusters of cancer cells must be primarily based on theoretical calculations. Howell et al. (7) have suggested that radionuclides which emit low-energy electrons (e.g., $^{193\text{m}}\text{Pt}$), with ranges in tissue of the order of the radius of the micrometastases, will deliver higher doses to the cluster than energetic beta emitters while only minimally irradiating the surrounding tissue. Similar advantages are expected from alpha emitters (8,9).

When radioimmunoconjugates are distributed in a micrometastasis, there are three contributions to the absorbed dose to a given cell in the cluster: (1) self-dose (sd), which results from the radionuclide localized in the same cell; (2) cross-dose (cd), which comes from the radiations emanating from all other cells in the cluster; and (3) the dose received from radioactivity distributed elsewhere (e.g., circulating antibody, etc.). The self-dose is highly dependent on the subcellular distribution of the radiochemical, and type and energy of the emissions (7,10). In contrast, the cross-dose is relatively independent of subcellular localization and primarily dependent on radiation properties. With so many different variables (particle energy, radiation type, cluster size, subcellular distribution, fraction of cells labeled) affecting the total dose that is likely to be given to the cells in a very small tumor, it is important to understand the role of these variables so that

Received Sept. 13, 1993; revision accepted Dec. 14, 1993.
For correspondence or reprints contact: Roger W. Howell, PhD, Assistant Professor of Radiology, University of Medicine and Dentistry of New Jersey, New Jersey Medical School, MSB F-451, 185 South Orange Ave., Newark, NJ 07103.

TABLE 1
Number of Cells in Close-Packed Multicellular Clusters

Cluster diameter (μm)	26	39	48	56	70	89	106	200	400
Number of cells in cluster	13	43	79	135	249	531	935	5979	47453

better approaches may be developed to treat micrometastases.

The present work systematically examines the self-dose and cross-dose contributions from intracellular radioactivity within small micrometastases. Model calculations are performed to obtain self-dose-to-cross-dose (sd/cd) ratios to cell nuclei in multicellular clusters ranging from 26 to 400 μm in diameter. The cells in the cluster are labeled with monoenergetic electron and alpha particle sources distributed uniformly in different cell compartments (cell surface, cytoplasm and nucleus). Similar calculations are also carried out for a variety of radionuclides including alpha, beta and Auger emitters. The effect of labeling only a fraction of the cells in the cluster is examined as well. These calculations show that under some circumstances, the mean absorbed dose to the multicellular cluster as a whole provides an adequate description of the dose received by the cell nuclei. Accordingly, self-absorbed fractions for monoenergetic electron and alpha emitters distributed uniformly in small spheres of unit density matter are also provided. In those instances where dosimetry at the cellular level is of importance, simple methods to estimate the mean absorbed dose to the cell nuclei of the labeled cells without resorting to complex modeling are discussed.

COMPUTATIONAL METHODS

Multicellular Cluster Model

Dosimetry modeling of cells in close-packed geometry has been a topic of interest for some time. Tislar-Lentulis et al. (11) used such a model to examine the microdosimetry of ^{239}Pu and ^{131}I . Sastry et al. (12) and Howell et al. (7) determined the optimal energy for RIT of micrometastases with electron emitters. A similar model was also employed by Makrigiorgos et al. (13) to investigate the dose enhancement observed for Auger emitters when individual cells within an organ accumulated large amounts of activity. Recently, Humm et al. (9) and Stinchcomb and Roeske (8) also applied a multicellular model for applications in RIT.

The model used in this work is adopted from the work of Sastry et al. (12) and Howell et al. (7). The spherical multicellular cluster is assumed to be a collection of cells in close-packed cubic geometry such that 74% of the cluster volume is occupied by the cells and 26% by the interstitial spaces. The cells are spherical with diameters of 10 μm and contain a concentric spherical nucleus 8 μm in diameter. Cluster diameters ranging from 26 μm to 400 μm are considered (Table 1). The cells, cell nuclei, and interstitial spaces are considered to be unit density matter (14). Radioactivity may be distributed uniformly in any one of the

following compartments: (1) throughout the cell (C); (2) cell surface (CS); (3) cytoplasm (Cy); or (4) nucleus (N). Following the MIRD Schema (15), the mean absorbed dose rate \bar{D} to target region k in the target cell in the cluster is given by

$$\bar{D}_{k \leftarrow h} = \frac{1}{m_k} \sum_i \Delta_i \left\{ a_h^{\text{self}}(\phi_{k \leftarrow h}^{\text{self}})_i + \sum_j a_{hj}^{\text{cross}}(\phi_{k \leftarrow hj}^{\text{cross}})_i \right\}, \quad \text{Eq. 1}$$

where m_k is the mass of the target region, Δ_i is the mean energy emitted per nuclear transition for the i th radiation component, and a_h^{self} and a_{hj}^{cross} are the activity in source region h of the target cell and "jth with nontarget cell," respectively. The absorbed fraction $(\phi_{k \leftarrow hj}^{\text{cross}})_i$ is the fraction of the i th energy component emitted by activity in source region h within the j th nontarget cell that is deposited in target region k in the target cell, and $(\phi_{k \leftarrow h}^{\text{self}})_i$ is the cellular self-absorbed fraction (10).

The absorbed fraction $\phi_{k \leftarrow h}$ is given by

$$\phi_{k \leftarrow h} = \int_0^\infty \psi_{k \leftarrow h}(x) \frac{dE_i}{dX} \Big|_{X(E_i) - x} dx, \quad \text{Eq. 2}$$

where $\psi_{k \leftarrow h}(x)$ is the geometric reduction factor, E_i is the initial energy of the i th particulate radiation component, $X(E_i)$ is the range of a particle of energy E_i , x is the distance traveled by the particle, and dE_i/dX is the stopping power of the particulate radiation. For electrons, Cole (14) experimentally determined that the electron energy E_e (keV) and range X (μm) in unit density matter are related by

$$E_e = 5.9(X + 0.007)^{0.565} + 0.00413X^{1.33} - 0.367. \quad \text{Eq. 3}$$

Differentiation of Equation 3 yields the energy loss expression for electrons

$$dE_e/dX = 3.333(X + 0.007)^{-0.435} + 0.0055X^{0.33}. \quad \text{Eq. 4}$$

Hence, $dE/dX|_{X(E_i) - x}$ is the energy loss expression (Equation 4) evaluated at ' $X(E_i) - x$ ', the residual range of the particle after passing a distance of x through the medium. For alpha particles, $E_\alpha = 390 X^{2/3}$ and $dE_\alpha/dX = 260 X^{-1/3}$ (10). Integration of Equation 2 using these energy loss expressions ensures that the dose calculation takes into account the changes in LET of the particles as they traverse the cells in the cluster.

The geometric factor $\psi_{k \leftarrow h}(x)$ is the mean probability that a randomly directed vector of length x starting from a random point within the source region h ends within the target region k (Fig. 1) (16). This algebraic form of the geometric factor depends on the radii of the cell R_C and cell nucleus R_N and the subcellular distribution of the radioactivity in the cells of the cluster. In our previous communication (10), the geometric factors $\psi_{k \leftarrow h}^{\text{self}}(x)$ used for calculating cellular absorbed-fractions $\phi_{k \leftarrow h}^{\text{self}}(x)$ were provided for radioactivity distributed in any one of four source regions h within the cell as listed above. Similarly, in the present work,

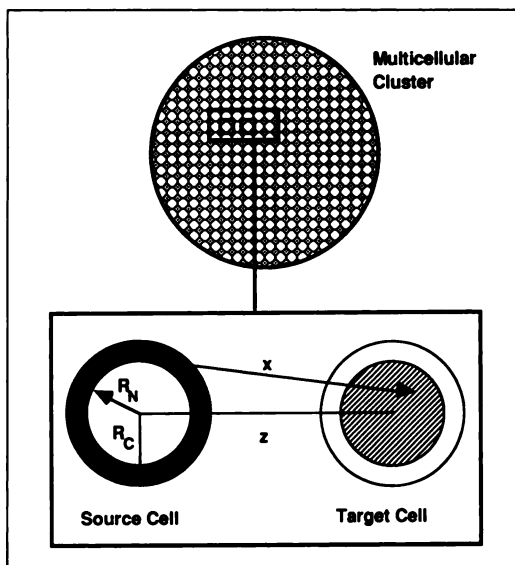


FIGURE 1. Geometry for cross-dose calculations in multicellular clusters. The radii of the cells (R_C) and cell nuclei (R_N) are $5 \mu\text{m}$ and $4 \mu\text{m}$, respectively. The parameter z is the distance between the centers of the cells, and x is a vector of length x that begins at a random point within the source region h (filled region) of the source cell and ends in the target region k (cross-hatched region) of the target cell.

the nontarget to target geometric factors $\psi_{k \leftarrow h}^{\text{cross}}(x)$ for calculating the cross-dose are given in the Appendix.

Absorbed fractions for electrons and alpha particles are calculated by numerical integration of Equation 2 using a FORTRAN 77 code running on a UNIX-based HP9000 series 800 computer. Dose rates to cells in the cluster are computed using Equation 1 and the calculated absorbed fractions.

Radionuclides and Radiation Spectra

Several radionuclides are considered in these model calculations. Auger electron emitters considered include ^{51}Cr , ^{67}Ga , $^{99\text{m}}\text{Tc}$, ^{111}In , ^{123}I , ^{125}I , ^{201}Tl , $^{193\text{m}}\text{Pt}$ and ^{203}Pb . The radiation spectra for these Auger emitters were taken from the recent AAPM Task Group Report (17). Calculations are also performed for the beta emitters ^{32}P , ^{35}S , ^{86}Rb , ^{89}Sr , ^{90}Y , ^{91}Y , $^{114\text{m}}\text{In}$, ^{131}I , ^{208}Tl and ^{212}Pb using radiation spectra from Weber et al. (18). Because use of the mean beta energy can introduce errors in cellular dosimetry (7,10), it is essential to use radiation spectra that reflect the continuous nature of the beta-spectrum. Browne et al. (19) have conveniently binned the beta-particle spectra in a logarithmic manner with respect to energy for all radionuclides. Hence, beta-particle components of Weber et al.'s spectra (18) are replaced with these. The final radionuclides considered are the alpha emitters ^{210}Po , ^{212}Bi and ^{212}Po (18). In addition to the numerous radionuclides considered above, multicellular dosimetry calculations are also carried out for hypothetical emitters of monoenergetic electrons (10 keV–1 MeV) or alpha particles (3–10 MeV).

Self-Absorbed Fractions and S-values for Small Spheres

Because complex multicellular dosimetry is sometimes not needed to adequately describe the dose received by the cells within a micrometastasis, it is useful to calculate self-absorbed fractions for uniform distributions of hypothetical monoenergetic electron and alpha emitters in small spheres (26–5000 μm in diameter). Similarly, S-values for a number of radionuclides are calculated for convenience. These calculations were performed using the computer code of Goddu et al. (10) which is valid for both cellular and macroscopic dimensions. Computational results were spot-checked against the code of Howell et al. (4).

RESULTS AND DISCUSSION

Alpha, beta and Auger emitters have all been promoted as candidates for radioimmunotherapy (2–4,6). The usefulness of each class of emitter largely depends on the size of the tumor, the fraction of cells labeled within the tumor, and the subcellular distribution of the radioactivity. The present multicellular model calculations permit an in-depth examination of the unique complications involved in the dosimetry of very small micrometastases.

Multicellular Dosimetry

The computational results presented in Figure 2 examine the dependence of the mean ratio of self-dose-to-cross-dose to the cell nucleus (sd/cd ratio) as a function of electron energy. The monoenergetic electron sources are assumed to be uniformly distributed in either the cytoplasm or nucleus of the cells, or on the cell surface. Each cell contains the same activity. It is clear that for large clusters ($d = 400 \mu\text{m}$), the self-dose contributes less than 10% of the total dose to the cell nucleus for electron energies greater than about 30 keV regardless of the subcellular distribution of the activity. This is largely true for the 106 μm cluster, with perhaps intranuclear localization of the radioactivity being the exception. Below 20–30 keV, the importance of the self-dose increases dramatically with it being the dominant contribution to the dose to the cell nucleus at energies less than 10 keV. Also shown in Figure 2 is the upward trend in sd/cd ratios as the size of the cluster decreases. For very small clusters (i.e., $<100 \mu\text{m}$), where the cross-fire is limited because of the small number of cells, the self-dose plays an important role for all subcellular distributions and all energies.

The results shown in Figure 3 for monoenergetic alpha particles are similar to those portions of the curves in Figure 2 for electrons having ranges of several cell diameters or more in unit density matter ($>50 \text{ keV}$). Because the range of the alpha particles is also several cell diameters, the cross-dose component of the dose to the cell nucleus is of greatest importance. In fact, the self-dose only plays a major role when the alpha emitter is localized in the cell nuclei of very small clusters (e.g., $\sim 26 \mu\text{m}$).

Figures 2 and 3 suggest that when 100% of the cells in the cluster are labeled, the self-dose is usually small for alpha

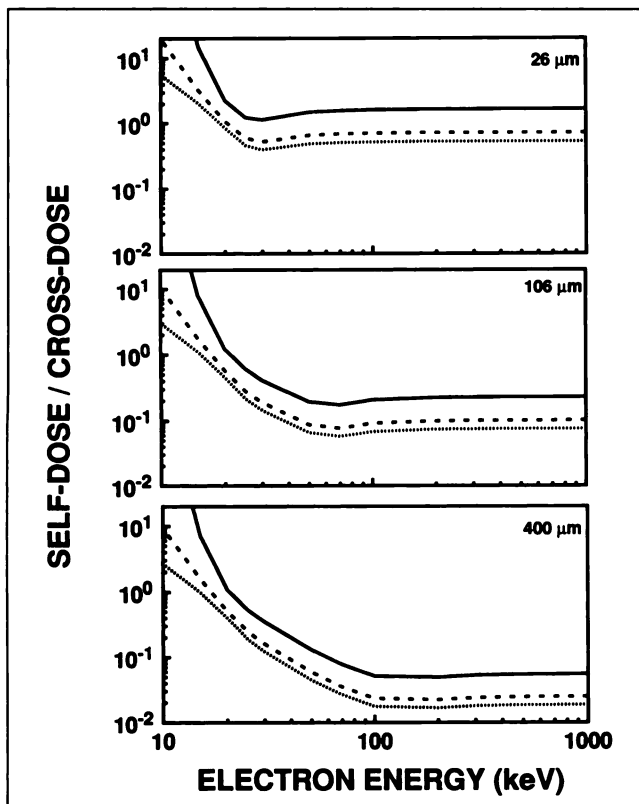


FIGURE 2. Dependence of the ratio of the self-dose-to-the cell nucleus to the mean cross-dose-to-the cell nucleus on electron energy. All cells in the multicellular cluster contain the same activity of a monoenergetic electron emitter that is uniformly distributed in either the cell nucleus (solid line), cytoplasm (dashed line) or on the cell surface (dotted line). Three different cluster diameters are considered (26 μm , 106 μm and 400 μm). Note that the self-dose dominates at low electron energies for all cluster sizes and all sub-cellular distributions. Furthermore, the self-absorbed dose plays a key role for all energies and all subcellular distributions when the cluster size is very small. As the cluster size increases, the role of the self-dose becomes minimal.

emitters and energetic electron emitters. However, it may be that only a fraction of cells in the cluster are labeled with radioactivity. Figure 4 shows dose profiles on a cell by cell basis as one moves across the cluster for three radionuclides (^{90}Y , ^{210}Po or ^{125}I) distributed uniformly in either the nucleus or on the cell surface. Either 1%, 10% or 100% of the cells in the 400- μm diameter cluster are randomly labeled. These radionuclides were selected as examples of beta, alpha and low-energy Auger electron emitters, respectively. Clearly, the subcellular distribution of the radionuclides and the self-dose play an increasingly important role in the dose profile as the fraction of cells that are labeled decreases. This is true for alpha, beta and Auger emitters alike, although the greatest effect on the dose profiles is seen for the Auger emitter ^{125}I . For example, when ^{90}Y is localized in the nucleus (cell surface) of only 1% of the cells, the labeled cells receive a dose 4–12 (2–5) times greater than the unlabeled cells. Factors of the order of 100 and 1000 are observed for ^{125}I when 10% and 1% of the cells are randomly labeled, respectively (Fig. 4). These

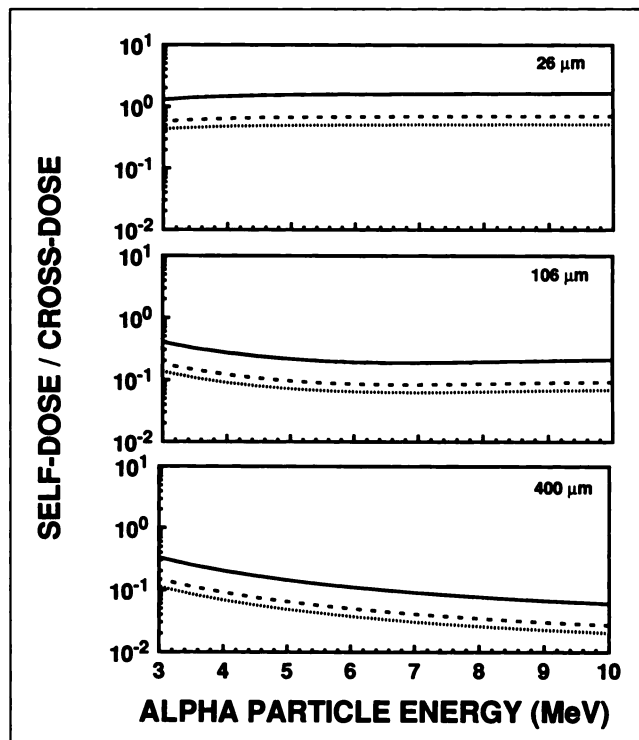


FIGURE 3. Ratio of the self-dose-to-the cell nucleus-to-the mean cross-dose-to-the cell nucleus as a function of alpha particle energy. Each cell in the multicellular cluster contains the same activity of a monoenergetic alpha particle emitter that is uniformly distributed in one of three cell compartments: cell nucleus (solid line), cytoplasm (dashed line) and cell surface (dotted line). Three different cluster diameters are considered (26 μm , 106 μm and 400 μm). Note that, in general, the self-dose does not constitute the major contribution to the total dose delivered to the cell nucleus.

calculations suggest that multicellular dosimetry may play a key role in RIT of micrometastases although we note that 1% labeling may not be likely in very small clusters.

Given the potential role of multicellular dosimetry in RIT, it is also interesting to examine the effect of cluster size on the sd/cd ratios. Figures 5–7 show the sd/cd ratios as a function of the cluster diameter for ^{90}Y , ^{210}Po and ^{125}I , respectively. In all three cases, the self-dose constitutes a major fraction of the total absorbed dose to the cell nuclei when 10% of the cells in the cluster are labeled, and sub-cellular distribution substantially impacts the sd/cd ratio in these cases. For 100% labeling, the self-dose is important only when the cluster diameter is very small, with the exception of the Auger emitter ^{125}I where the self-dose is nearly always significant. Because of the importance of the self-dose in the case of Auger emitters, sd/cd ratios for cell surface distribution $F_{N \leftarrow CS}$ are provided in Table 2 for 100% labeling with several common radionuclides of this type including ^{51}Cr , ^{67}Ga , $^{99\text{m}}\text{Tc}$, ^{111}In , ^{123}I , ^{125}I , $^{193\text{m}}\text{Pt}$, ^{201}Tl and ^{203}Pb . There are substantial variations in the ratios between the various Auger emitters which are due to the marked differences in the details of their radiation spectra (17). In addition, the cluster size has a pronounced impact on the sd/cd ratio. The diameter of the cell and cell

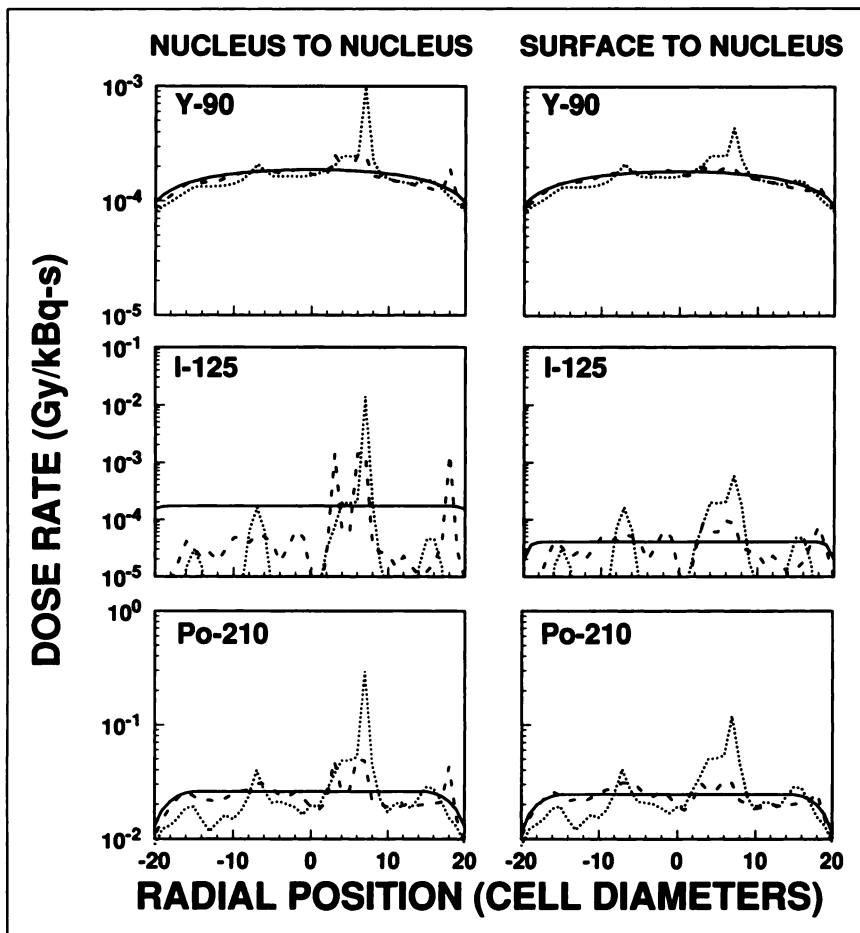


FIGURE 4. Dose-rate profiles in 400- μm diameter multicellular clusters containing 1 kBq of either ^{90}Y , ^{210}Po or ^{125}I . The radioactivity is uniformly distributed either in the cell nucleus (left) or on the cell surface (right), and the radioactivity is confined to 1% (dotted line), 10% (dashed line) or 100% (solid line) of the cells in the cluster at random. The spikes observed for the 1% and 10% labeling cases correspond to cells that are labeled. The increasing importance of the subcellular distribution and the self-dose is apparent as the percentage of cells that are labeled decreases, particularly for the Auger emitter ^{125}I .

nucleus may have a substantial effect as well (9). The tabulated ratios $F_{N \rightarrow CS}$ for cell surface distribution are relatively small and range from about 0.02 to about 2.7. With the exception of ^{51}Cr , the sd/cd ratios for cytoplasmic localization $F_{N \rightarrow Cy}$ are about two times larger than the ratios for surface distribution $F_{N \rightarrow CS}$ (Table 2, last column). The highly localized nature of energy deposition by Auger emitters (20) is clearly indicated in column 7 of Table 2. When Auger emitters are localized in the nucleus of the cells in the cluster, the sd/cd ratios are enhanced by about 8–35 times compared to localization on the cell surface. The enhancement for ^{51}Cr (85,000) is much greater because most of the electrons emitted have very short ranges ($<1 \mu\text{m}$) and therefore the cross-dose contribution is negligible. The therapeutic gain realized by introducing these radionuclides into the nucleus is apparent. This gain may be further enhanced by up to a factor of 10 due to the high values of relative biological effectiveness (RBE) of Auger emitters when localized in the cell nucleus (21–25).

The above examination of the dependence of the sd/cd ratios on a variety of parameters provides insight into the relative importance of the self-dose and cross-dose in RIT of micrometastases. However, it is the absorbed dose to the cell nuclei of the cluster that is of principal importance. The sd/cd ratios presented in Table 2 and Figures 2, 3 and 5–7 may be

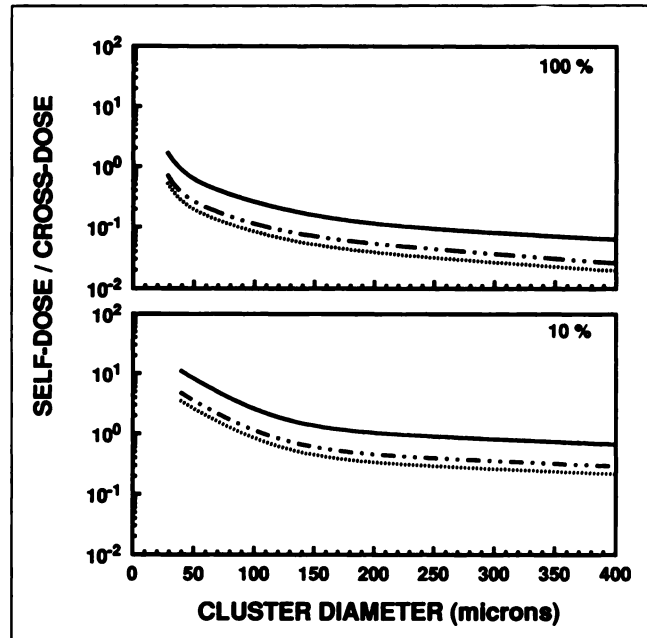


FIGURE 5. Ratio of the self-dose-to-the cell nucleus-to-the mean cross-dose-to-the cell nucleus as a function of multicellular cluster diameter for the high-energy beta emitter ^{90}Y . The radioactivity is uniformly distributed in either the cell nucleus (solid line), cytoplasm (dashed line) or cell surface (dotted line), and is confined to 10% or 100% of the cells in the cluster. These curves show that the self-dose can be significant for beta emitters when the cluster diameter is small and when only a small fraction of the cells are labeled.

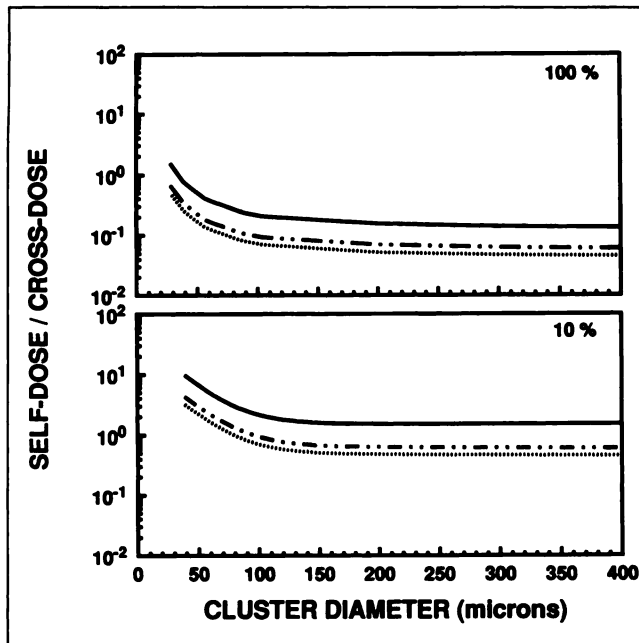


FIGURE 6. Ratio of the self-dose-to-the cell nucleus-to-the mean cross-dose-to-the cell nucleus as a function of multicellular cluster diameter for the alpha emitter ^{210}Po . The radioactivity is uniformly distributed in either the cell nucleus (solid line), cytoplasm (dashed line) or cell surface (dotted line), and is confined to 10% or 100% of the cells in the cluster. These curves are very similar to those obtained for the beta emitter ^{90}Y and show that the self-dose is significant for alpha emitters when the cluster diameter is small and when only a small fraction of the cells are labeled.

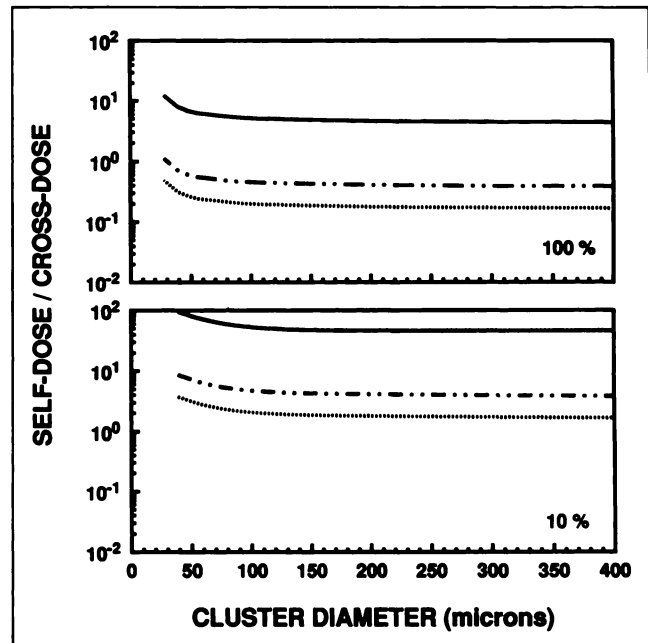


FIGURE 7. Ratio of the self-dose-to-the cell nucleus-to-the mean cross-dose-to-the cell nucleus as a function of multicellular cluster diameter for the Auger emitter ^{125}I . The radioactivity is uniformly distributed in either the cell nucleus (solid line), cytoplasm (dashed line) or cell surface (dotted line), and is confined to 10% or 100% of the cells in the cluster. The self-dose always constitutes a significant fraction of the total absorbed dose to the cell nucleus for Auger emitters.

used to calculate the total mean absorbed dose (self-dose + cross-dose) to the cell nuclei of the labeled cells $\bar{D}_{N \leftarrow h}$.

$$\bar{D}_{N \leftarrow h}^{\text{total}} = \bar{A}_h^{\text{self}} S_{N \leftarrow h}^{\text{self}} \left(1 + \frac{1}{F_{N \leftarrow h}} \right). \quad \text{Eq. 5}$$

The quantities \bar{A}_h^{self} and $S_{N \leftarrow h}^{\text{self}}$ are the mean cumulated activity in a labeled cell and the cellular S-value (10), respectively. The cellular S-values are tabulated conveniently in our earlier report for a number of radionuclides (10). As an example of calculating the mean absorbed dose

to the cell nuclei using Equation 5, consider a 200- μm diameter cluster containing ^{125}I uniformly distributed on the surface of the cells ($R_C = 5 \mu\text{m}$, $R_N = 4 \mu\text{m}$). Taking $F_{N \leftarrow CS} (^{125}\text{I}) = 0.0983$ from Table 2 and $S_{N \leftarrow CS}^{\text{self}} = 1.40 \times 10^{-4} \text{ Gy/Bq} \cdot \text{s}$ from Goddu et al. (10), one obtains $1.56 \times 10^{-3} \bar{A}_h^{\text{self}}$. The mean dose to the cell nuclei for surface distribution is then $1.56 \times 10^{-3} \text{ Gy}$ per unit cumulated activity in the cell ($\text{Bq} \cdot \text{s}$). Similar calculations may be performed for alpha and beta emitters using the sd/cd ratios in Figures 2 and 3 and the S-values (10).

Although calculation of cellular doses within multicellu-

TABLE 2
Self-Dose-to-Cross-Dose Ratios for Auger Electron Emitters

Radionuclide	Self-dose-to-cross-dose ratios ($F_{N \leftarrow CS}$)					Approximate subcellular distribution enhancement factor	
	26 μm	48 μm	106 μm	200 μm	400 μm	$F_{N \leftarrow N} / F_{N \leftarrow CS}$	$F_{N \leftarrow O} / F_{N \leftarrow CS}$
^{51}Cr	0.527	0.203	0.0738	0.0376	0.0180	85000	5850
^{67}Ga	1.40	0.543	0.182	0.0877	0.0604	14	2.5
^{99m}Tc	0.789	0.332	0.127	0.0615	0.0290	35	1.9
^{111}In	0.792	0.442	0.254	0.162	0.0868	15	1.6
^{123}I	0.531	0.284	0.158	0.0983	0.0528	21	1.9
^{125}I	0.482	0.263	0.193	0.175	0.174	25	2.3
^{183m}Pt	1.84	0.769	0.292	0.157	0.0796	12	2
^{201}Tl	1.47	0.691	0.313	0.198	0.146	14	2
^{203}Pb	2.67	1.17	0.467	0.269	0.145	20	2.5

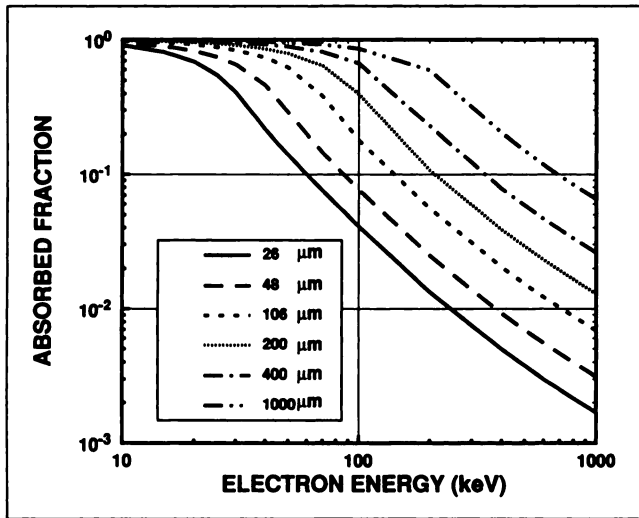


FIGURE 8. Absorbed fractions for sources of monoenergetic electrons distributed uniformly in spheres of unit density matter.

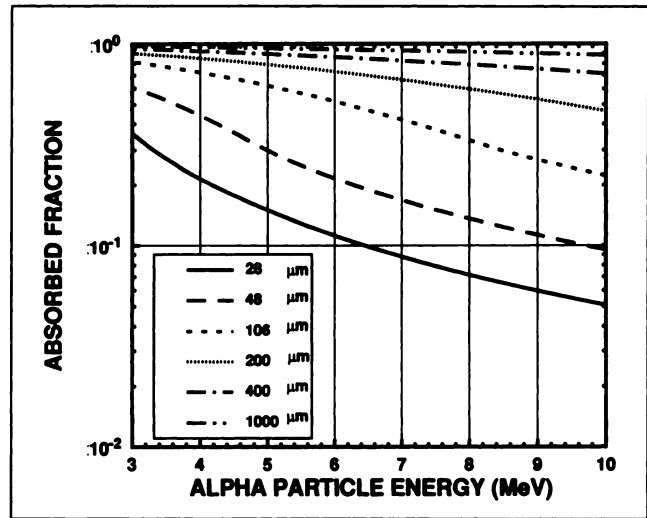


FIGURE 9. Absorbed fractions for uniform distribution of monoenergetic alpha particle sources in spheres of unit density matter.

lar cluster models sheds light on a number of important dosimetric considerations, the application of such calculations to predict biologic effect (e.g., eradication of the micrometastases) remains tenuous. Calculation of the absorbed doses received by the cells within an in vivo micrometastasis requires detailed information on the geometry of the cluster, as well as biokinetic data on the uptake, clearance and subcellular distribution of radioactivity within each cell of the cluster. To further complicate matters, subcellular distribution may vary with time. These data are clearly difficult to acquire, particularly for the very

small metastases that are the topic of this work. Some strides have been made, however, in gathering some of the needed in vivo data using quantitative autoradiographic techniques (26–28). Correlation of the doses calculated from these data with the biologic effect remains a challenge (29).

Macroscopic Dosimetry

In those instances where the self-dose plays little or no role, the mean absorbed dose to the cell nuclei is essentially equal to the mean absorbed dose to the microme-

TABLE 3
S-values for Spheres Containing Uniformly Distributed Activity

Radionuclide	S-Value (Gy/Bq · s)						
	26 μm	48 μm	106 μm	200 μm	400 μm	1000 μm	5000 μm
³² P	3.59E-05	1.04E-05	2.12E-06	5.86E-07	1.44E-07	2.28E-08	7.59E-10
³⁵ S	1.32E-04	3.29E-05	5.55E-06	1.17E-06	1.85E-07	1.36E-08	1.16E-10
⁵¹ Cr	6.23E-05	9.99E-06	9.33E-07	1.39E-07	1.74E-08	1.12E-09	9.04E-12
⁶⁷ Ga	1.29E-04	2.45E-05	3.33E-06	7.71E-07	1.26E-07	9.39E-09	8.12E-11
⁸⁶ Rb	4.02E-05	1.15E-05	2.31E-06	6.28E-07	1.50E-07	2.32E-08	7.13E-10
⁸⁹ Sr	4.10E-05	1.17E-05	2.35E-06	6.37E-07	1.52E-07	2.35E-08	7.12E-10
⁹⁰ Y	3.53E-05	1.02E-05	2.07E-06	5.71E-07	1.39E-07	2.19E-08	7.56E-10
⁹¹ Y	4.06E-05	1.16E-05	2.33E-06	6.33E-07	1.51E-07	2.34E-08	7.14E-10
^{90m} Tc	5.25E-05	9.37E-06	1.12E-06	2.36E-07	4.79E-08	4.14E-09	3.81E-11
¹¹¹ In	1.08E-04	1.95E-05	2.16E-06	3.97E-07	7.22E-08	7.45E-09	7.91E-11
^{114m} In	1.34E-04	3.18E-05	5.45E-06	1.42E-06	3.53E-07	5.07E-08	1.05E-09
¹²³ I	1.15E-04	2.11E-05	2.39E-06	4.49E-07	8.28E-08	7.05E-09	6.48E-11
¹²⁵ I	2.53E-04	4.59E-05	4.66E-06	7.17E-07	9.13E-08	5.91E-09	4.75E-11
¹³¹ I	8.37E-05	2.25E-05	4.20E-06	1.03E-06	2.16E-07	2.80E-08	4.01E-10
^{193m} Pt	4.15E-04	7.73E-05	9.84E-06	2.04E-06	4.07E-07	3.50E-08	3.22E-10
²⁰¹ Tl	2.97E-04	5.39E-05	6.34E-06	1.17E-06	1.74E-07	1.27E-08	1.09E-10
²⁰³ Pb	1.71E-04	2.94E-05	3.19E-06	5.65E-07	9.28E-08	1.00E-08	1.16E-10
²⁰⁸ Tl	4.52E-05	1.29E-05	2.59E-06	7.05E-07	1.69E-07	2.61E-08	7.43E-10
²¹⁰ Po	1.25E-02	3.93E-03	8.04E-04	1.57E-04	2.24E-05	1.54E-06	1.28E-08
²¹² Pb	1.92E-04	4.53E-05	7.53E-06	1.78E-06	3.80E-07	4.26E-08	5.32E-10
²¹² Bi	4.26E-03	1.30E-03	2.90E-04	6.10E-05	9.04E-06	6.41E-07	5.71E-09
²¹² Po	9.46E-03	2.84E-03	6.30E-04	1.83E-04	3.19E-05	2.42E-06	2.10E-08

tastasis as a whole. Hence, the complex multicellular structure may be abandoned in these instances and the self-dose to the sphere may be calculated using conventional techniques (15). However, there is little information available on absorbed fractions for particulate radiation emitted from very small volumes. Accordingly, absorbed fractions for a uniform distribution of monoenergetic electron sources in homogeneous spheres of unit density matter are given in Figure 8 to facilitate absorbed dose calculations for micrometastases. Data are provided in Figure 9 for monoenergetic alpha sources. For convenience, S-values for calculation of self-absorbed doses to spherical regions containing uniformly distributed radioactivity are given in Table 3 for a number of radionuclides.

SUMMARY

The computational results described in the present work provide guidance with regard to the dosimetry of very small micrometastases. The relative importance of the self-dose and cross-dose delivered to the nuclei of the cells in the cluster depends strongly on the type of radionuclide (alpha, beta and Auger), cluster diameter, subcellular distribution and fraction of cells that are labeled. In general, the cellular self-dose plays a primary role when Auger emitters are used to treat micrometastases. However, the cross-dose frequently constitutes the majority of the dose

delivered by alpha and beta emitters. The exceptions to this are when the cluster diameter is very small ($<50 \mu\text{m}$) or when only a small fraction of the cells in the cluster are labeled. When the cross-dose dominates, the mean absorbed dose to the cell nuclei in the cluster is reasonably well represented by the mean absorbed dose to the cluster as a whole. Although many of the salient aspects of the dosimetry of micrometastases have been addressed here, other factors may need to be taken into account such as nonuniform distributions of activity in the cluster (7), cluster growth (30), cell size (9) and microdosimetric considerations (8,31,32). Finally, relating the absorbed doses calculated at the cellular level to observed biological effects (i.e., sterilization of the micrometastasis) may be difficult and must account for dose rate effects (2,33) and RBE if alpha or Auger emitters (21,23-25,34) are involved.

APPENDIX

The geometric factors $\psi_{k \leftarrow h}^{\text{self}}(x)$ used for calculating the self-absorbed fraction for radioactivity within the cell were provided in an earlier article (10). The geometric factors $\psi_{k \leftarrow h}^{\text{cross}}(x)$ used for calculating the dose from neighboring cells (cross-dose) are given below. Figure 1 shows the geometry of the source and target cell within the multicellular cluster. When radioactivity is distributed uniformly on the cell surface (CS) of the source cells, the geometric factor for the target cell nucleus (N) is given by

$$\psi_{N \leftarrow \text{CS}}^{\text{cross}}(x) = \begin{cases} 0 & \text{when } x \leq z - R_C - R_N \\ -W[x^3 + 3x^2(R_C - z) + 3x(R_C^2 - 2zR_C + z^2 - R_N^2) - 2R_N^3 + R_C^3 - 3zR_C^2 + 3R_C(z^2 - R_N^2) - z^3 + 3R_N^2z] & \text{when } z - R_C - R_N \leq x \leq z - R_C + R_N \\ 4WR_N^3 & \text{when } R_C \neq R_N \\ & \text{and } z - R_C + R_N \leq x \leq z + R_C - R_N \\ -W[-x^3 + 3x^2(R_C + z) + 3x(-R_C^2 - 2zR_C - z^2 + R_N^2) - 2R_N^3 + R_C^3 + 3zR_C^2 + 3R_C(z^2 - R_N^2) + z^3 - 3R_N^2z] & \text{when } z - R_N + R_C \leq x \leq z + R_N + R_C \\ 0 & \text{when } x \geq z + R_N + R_C \end{cases} \quad \text{Eq. A1}$$

where z is the distance between the centers of the source and target cells (Fig. 1), x is the distance from a random point within the source region to a random point in the target region, and $W = 1/(24zxR_C)$. The parameters R_C and R_N are the radii of the cell and cell nucleus, respectively. When the entire cell is taken as the target region, the geometric factor $\psi_{C \rightarrow CS}^{\text{cross}}(x)$ may be obtained by substituting R_C for R_N in the above equation. These geometric factors, which depend only on z , x , R_C and R_N , are relevant for any given pair of source and target cells and are therefore independent of the manner in which the cells are packed into the multicellular cluster (e.g., hexagonal, body-centered cubic, etc.).

When the radioactivity is distributed uniformly throughout the source cell (C) and the nucleus of the target cell is taken as the target region, the geometric factor $\psi_{N \rightarrow C}^{\text{cross}}(x)$ is given by

$$\psi_{N \rightarrow C}^{\text{cross}} = \begin{cases} 0 & \text{when } x \leq z - R_C - R_N \\ Y [x^5 - 5zx^4 + 10x^3(z^2 - R_C^2 - R_N^2) \\ + 10x^2(3R_N^2z - 2R_N^3 - 2R_C^3 + 3R_C^2z - z^3) \\ + 5x(6R_N^2R_C^2 - 6R_N^2z^2 + 8R_N^3z - 3R_N^4 \\ - 3R_C^4 + 8zR_C^3 - 6R_C^2z^2 + z^4) \\ - 4R_C^5 + 15zR_C^4 - 20R_C^3(z^2 - R_N^2) \\ + 10R_C^2(2R_N^3 + z^3 - 3zR_N^2) \\ - z^5 + 10R_N^2z^3 - 20R_N^3z^2 + 15R_N^4z - 4R_N^5] & \text{when } z - R_C - R_N \leq x \leq z - R_C + R_N \\ 8YR_N^3[-5x^2 + 10zx + 5R_C^2 - 5z^2 - R_N^2] & \text{when } z - R_C + R_N \leq x \leq z - R_N + R_C \\ -Y [x^5 - 5zx^4 + 10x^3(z^2 - R_C^2 - R_N^2) \\ + 10x^2(3R_N^2z + 2R_N^3 + 2R_C^3 + 3R_C^2z - z^3) \\ + 5x(6R_N^2R_C^2 - 6R_N^2z^2 - 8R_N^3z - 3R_N^4 \\ - 3R_C^4 - 8zR_C^3 - 6R_C^2z^2 + z^4) \\ + 4R_C^5 + 15zR_C^4 + 20R_C^3(z^2 - R_N^2) \\ + 10R_C^2(-2R_N^3 + z^3 - 3zR_N^2) \\ - z^5 + 10R_N^2z^3 + 20R_N^3z^2 + 15R_N^4z + 4R_N^5] & \text{when } z - R_N + R_C \leq x \leq z + R_N + R_C \\ 0 & \text{when } x \geq z + R_N + R_C \end{cases}$$

Eq. A2

where $Y = 1/160zxR_C^3$. The geometric factors $\psi_{N \rightarrow N}^{\text{cross}}(x)$ and $\psi_{C \rightarrow C}^{\text{cross}}(x)$ may be obtained by substituting R_N for R_C and R_C for R_N , respectively, in the above expression for $\psi_{N \rightarrow C}^{\text{cross}}(x)$.

The expressions above may be used with Equation 2 to directly calculate the absorbed fractions $\phi_{C \rightarrow C}^{\text{cross}}(x)$, $\phi_{C \rightarrow CS}^{\text{cross}}(x)$, $\phi_{N \rightarrow N}^{\text{cross}}(x)$, and $\phi_{N \rightarrow CS}^{\text{cross}}(x)$. Using the reciprocity theorem (15), one may obtain the quantity $\phi_{N \rightarrow Cy}^{\text{cross}}(x)$ from the above absorbed fractions.

$$\phi_{N \rightarrow Cy}^{\text{cross}} = \frac{m_N}{m_{Cy}} \left(\frac{m_C}{m_N} \phi_{N \rightarrow C}^{\text{cross}} - \phi_{N \rightarrow N}^{\text{cross}} \right) \quad \text{Eq. A3}$$

The quantities m_{Cy} , m_N and m_C are the mass of the cytoplasm, nucleus and cell, respectively. It should be noted that when the source and target cell are separated by more than a few cell diameters, the quantities $\phi_{N \rightarrow N}^{\text{cross}}(x)$, $\phi_{N \rightarrow CS}^{\text{cross}}(x)$, and $\phi_{N \rightarrow Cy}^{\text{cross}}(x)$ are usually

approximately equal to one another. That is, the cross-dose to the target cell is not strongly affected by the subcellular distribution of the radionuclide in the source cell when the separation between the source and target cells is more than a few cell diameters. The separation distance at which the difference in these quantities becomes negligible depends primarily on the diameters of the cell and cell nucleus, and the range of the emitted radiations.

ACKNOWLEDGMENTS

The authors thank Chris Haydock for his contribution in the derivation of the geometric factors. This work was supported in part by USPHS grants CA-32877 and CA-54891 and a grant 26-93 from the UMDNJ Foundation.

REFERENCES

- Siegel JA, Pawlyk DA, Lee RE, et al. Tumor, red marrow, and organ dosimetry for ^{131}I -labeled anti-carcinoembryonic antigen monoclonal antibody. *Cancer Res* 1990;50(Suppl):1039s-1042s.
- Rao DV, Howell RW. Time dose fractionation in radioimmunotherapy: Implications for selecting radionuclides. *J Nucl Med* 1993;34:1801-1810.
- Wessels BW, Rogus RD. Radionuclide selection and model absorbed dose calculations for radiolabeled tumor associated antibodies. *Med Phys* 1984; 11:638-645.
- Howell RW, Rao DV, Sastry KSR. Macroscopic dosimetry for radioimmunotherapy: nonuniform activity distributions in solid tumors. *Med Phys* 1989;16:66-74.
- Mausner LF, Srivastava SC. Selection of radionuclides for radioimmunotherapy. *Med Phys* 1993;20(part 2):503-509.
- Humm JL. Dosimetric aspects of radiolabeled antibodies for tumor therapy. *J Nucl Med* 1986;27:1490-1497.
- Howell RW, Rao DV, Haydock C. Dosimetry techniques for therapeutic applications of incorporated radionuclides. In: Adelstein SJ, Kassis AI, Burt RW, eds. *Dosimetry of administered radionuclides*. Washington, DC: American College of Nuclear Physicians; 1990:215-256.
- Stinchcomb TG, Roeske JC. Analytic microdosimetry for radioimmunotherapeutic alpha emitters. *Med Phys* 1992;19:1385-1393.
- Humm JL, Cobb LM. Nonuniformity of tumor dose in radioimmunotherapy. *J Nucl Med* 1990;31:75-83.
- Goddu SM, Howell RW, Rao DV. Cellular dosimetry: absorbed fractions for monoenergetic electron and alpha particle sources, and S-values for radionuclides, distributed uniformly in different cell compartments. *J Nucl Med* 1993;35:303-316.
- Tisljar-Lentulis G, Feinendegen LE, Walther H. Calculation of specific energies of incorporated ^{239}Pu and ^{131}I in accordance with the concept of the critical cell. *Radiat Envir Biophys* 1976;13:197-204.
- Sastry KSR, Haydock C, Basha AM, Rao DV. Electron dosimetry for radioimmunotherapy: optimal electron energy. *Radiat Prot Dosim* 1985;13: 249-252.
- Makrigiorgos GM, Adelstein SJ, Kassis AI. Limitations of conventional internal dosimetry at the cellular level. *J Nucl Med* 1989;30:1856-1864.
- Cole A. Absorption of 20 eV to 50,000 eV electron beams in air and plastic. *Radiat Res* 1969;38:7-33.
- Loevinger R, Budinger TF, Watson EE. *MIRD primer for absorbed dose calculations, revised*. New York: The Society of Nuclear Medicine; 1991.
- Berger MJ. Beta-ray dosimetry calculations with the use of point kernels. In: Cloutier RJ, Edwards CL, Snyder WS, eds. *Radiation dose and effects*. Washington, DC: U.S. Atomic Energy Commission; 1970:63-86.
- Howell RW. Radiation spectra for Auger-electron emitting radionuclides: report no. 2 of AAPM Nuclear Medicine Task Group no. 6. *Med Phys* 1992;19:1371-1383.
- Weber DA, Eckerman KF, Dillman LT, Ryman JC. *MIRD: radionuclide data and decay schemes*. New York: Society of Nuclear Medicine; 1989.
- Browne E, Firestone RB. *Table of radioactive isotopes*. New York: Wiley; 1986.
- Sastry KSR, Rao DV. Dosimetry of low energy electrons. In: Rao DV, Chandra R, Graham M, eds. *Physics of nuclear medicine: recent advances*. New York: American Institute of Physics; 1984:169-208.
- Rao DV, Sastry KSR, Grimmond HE, et al. Cytotoxicity of some indium radiopharmaceuticals in mouse testes. *J Nucl Med* 1988;29:375-384.
- Rao DV, Narra VR, Howell RW, Sastry KSR. Biological consequence of nuclear versus cytoplasmic decays of ^{125}I : cysteamine as a radioprotector against Auger cascades in vivo. *Radiat Res* 1990;124:188-193.
- Sastry KSR. Biological effects of the Auger emitter ^{125}I : a review. Report no. 1 of AAPM Nuclear Medicine Task Group no. 6. *Med Phys* 1992;19: 1361-1370.
- Howell RW, Narra VR, Sastry KSR, Rao DV. On the equivalent dose for Auger electron emitters. *Radiat Res* 1993;134:71-78.
- Howell RW, Rao DV, Hou D-Y, Narra VR, Sastry KSR. The question of relative biological effectiveness and quality factor for Auger emitters incorporated into proliferating mammalian cells. *Radiat Res* 1991;128:282-292.
- Jönsson B-A, Strand S-E, Larsson BS. A quantitative autoradiographic study of the heterogeneous activity distribution of different indium-111-labeled radiopharmaceuticals in rat tissues. *J Nucl Med* 1992;33:1825-1832.
- Roberson PL. Quantitative autoradiography for the study of radiopharmaceutical uptake and dose heterogeneity. *J Nucl Med* 1992;33:1833-1835.
- Roberson PL, Buchsbaum DJ, Heidorn DB, Ten Haken RK. Three-dimensional tumor dosimetry for radioimmunotherapy using serial autoradiography. *Int J Radiat Oncol Biol Phys* 1992;24:329-334.
- Humm JL, Chin LM. A model of cell inactivation by alpha-particle internal emitters. *Radiat Res* 1993;134:143-150.
- Howell RW, Narra VR, Rao DV. Absorbed dose calculations for rapidly growing tumors. *J Nucl Med* 1992;33:277-281.
- Humm JL, Roeske JC, Fisher DR, Chen GTY. Microdosimetric concepts in radioimmunotherapy. *Med Phys* 1993;20(part 2):535-541.
- Fisher DR, Frazier ME, Andrews JTK. Energy distribution and the relative biological effects of internal alpha emitters. *Radiat Prot Dosim* 1985;13:223-227.
- Langmuir VK, Fowler JF, Knox SJ, Wessels BW, Sutherland RM, Wong JYC. Radiobiology of radiolabeled antibody therapy as applied to tumor dosimetry. *Med Phys* 1993;20:601-610.
- Kassis AI, Howell RW, Sastry KSR, Adelstein SJ. Positional effects of Auger decays in mammalian cells in culture. In: Baverstock KF, Charlton DE, eds. *DNA damage by Auger emitters*. London: Taylor & Francis; 1988:1-14.